  Bull. Chem. Soc. Jpn., 64, 2207—2213 (1991)

VUV Photoionization Efficiency Curves and Appearance Energies of *N*, *N*-Dimethylformamide Ion and Its Fragment Ions

Masana ARIMURA* and Yozaburo YOSHIKAWA
Institute of Chemistry, College of General Education, Osaka University,
1-1 Machikaneyama, Toyonaka, Osaka 560
(Received December 28, 1990)

Ionization efficiency curves of *N*,*N*-dimethylformamide (DMF) ion and of its fragment ions, $C_3H_6NO^+$, $C_2H_4NO^+$, and $C_2H_6N^+$ were obtained by use of vacuum ultraviolet photoionization method. The appearance energy of the parent ion was 9.12±0.06 eV. The appearance energies of $C_3H_6NO^+$, $C_2H_4NO^+$, and $C_2H_6N^+$ were very close (10.77±0.08 eV for $C_3H_6NO^+$ and $C_2H_4NO^+$, 10.59±0.08 eV for $C_2H_6N^+$). The relative intensity curve of $C_2H_6N^+$ normalized by the sum of fragment ions vs. photon energy has the second rise at 12.2±0.3 eV, which implies that another fragmentation process appears at the photon energy above 12.2 eV. The second fragmentation process is ascribed to a channel through DMF cation in an excited electronic state.

Determination of the ionization energy of a parent molecule and appearance energies of its fragment ions is most important to elucidate the fragmentation mechanism and their reactions with other molecules. Several methods have been carried out to determine the ionization energy of a molecule and appearance energies of its fragment ions.[1] By using a photoionization technique, ionization energies of molecules are determined from the photon energy at which the ion current vanishes. This method is also useful for the estimation of appearance energies of the fragment ions which are produced through processes faster than ca. 10^4 sec^{-1} in the vicinity of critical energies.

Most of unimolecular reactions of the parent and fragment ions have been examined mainly in term of statistical partitioning of the whole energy to the vibration and rotation modes. Fragmentation rates are successfully understood by means of the statistical RRKM theory.[2] It has been reported that the statistical theory, however, can not be applied to the fragmentations of small molecular ions and fragmentations via the stable isomers of parent ion.[3] On the high energy excitation, another kind of unimolecular reactions, which the statistical theory failed to explain, occurs from electronic excited states before converting the electronic energy to the vibrational energy of ground state.[4]

Participation of another process is expected to emerge as another rise in the relative intensity curve normalized by the sum of the fragment ions (RI curve) which is derived from the ionization efficiency curves. We have found by using vacuum ultraviolet (VUV) photoionization technique that the CHO· elimination reaction of DMF cation exhibits plural thresholds at 10.59 eV and 12.2 eV of photon energy and that the fragmentations eliminating $C_3H_6NO^+$, $C_2H_4NO^+$, and $C_2H_6N^+$ appear at nearly the same energy. Ionization efficiency curves of DMF and the RI curves of the fragment ions were utilized to elucidate the fragmentation mechanisms.

Experimental

Photoionization efficiency curves were obtained by using a quadrupole mass spectrometer (QMS; Extranucler Co.). The mass resolution (ΔM) of QMS was ca. 1 (about 10 channels per mass unit for measurement).[5] An H_2 discharge lamp was used as the VUV light source for the ionization. The H_2 discharge lamp was operated at about 1 kW with 20—25 A cm^{-2} of current. The wavelength resolution of a monochrometor (McPherson model 234) is 8 Å full width at half maximum (FWHM), or ca. 0.07 eV in the energy range covered when the width and length of both entrance and exit slits are 100 μm and 3 mm respectively. The wavelength of light beam was calibrated by Lyman α line (1216 Å). The light beam strikes a thin layer of sodium salicylate as phosphor after traversing the ionization chamber. The fluorescence was led through an optical fiber to a photonmultiplier to obtain the photon intensity. The ions were counted by using a secondary electron multiplier (Ceratoron, Murata Seisakusyo). Values of ion-counting were given as the sum of the counted number of ions at three points (the peak top, before and behind the peak top of the resolved mass peak). The measurements of the ionization efficiency curves were fully operated by using a microcomputer. The light wavelength was scanned by 3 Å step for the measurements. The sample gas was introduced into the ion source without temperature control through a variable leak valve (the sample stagnation pressure was its vapor pressure at 0 °C).

The pressure of the vaccum chamber was measured intermittently by an ionization gauge just above the QMS and was held lower than 8×10^{-6} Torr (1 Torr=133.322 Pa).

The ionization energy 9.24±0.06 eV of benzene obtained here (Fig. 1) agrees very closely with the data obtained by others.[6]

The fragment ions were assigned by using a high resolution electron impact mass spectrometer (JMS-01SG-2, JEOL Co) at ca. 15 eV electron energy.

Results

Photoionization efficiency curves of DMF ion, m/z 73, and of its fragment ions, m/z 72, 58, and 44, were obtained in the photon energy range of 8.85—13.0 eV (Fig. 2). The other fragment ion in this energy region is mainly m/z 30.

The RI curves for the four fragment ions were obtained from the ionization efficiency curves, as are shown in Fig. 3. The RI curves give the relative fragmentation rates which are the convoluted rate from the critical photon

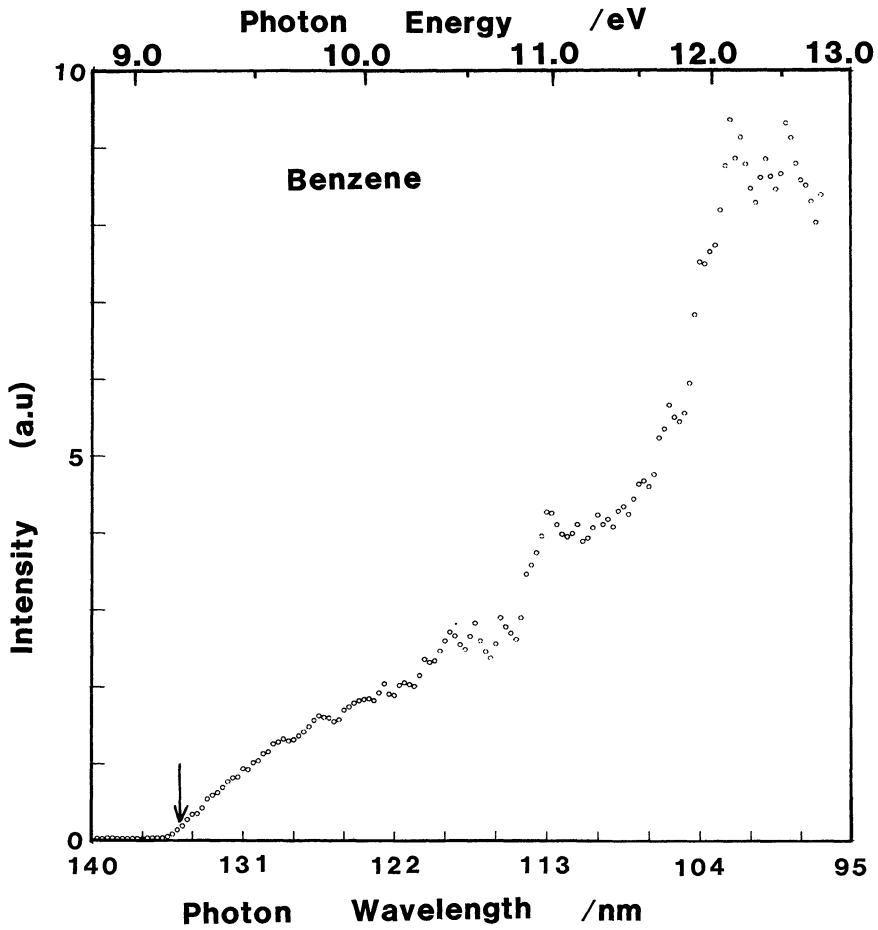

Fig. 1. The photoionization efficiency curve of benzene. The arrow shows the vertical ionization energy, 9.24±0.06 eV.

Table 1. Ionization and Appearance Energy of *N,N*-Dimethylformamide and Its Fragments (eV)

	This work (PI)	Reference
$C_3H_7NO^+$	9.12±0.06	9.12±0.02 (PI)[a] 9.14 (PE)[b]
$C_3H_6NO^+$	10.77±0.08	—
$C_2H_4NO^+$	10.77±0.08	—
$C_6H_6N^+$	10.59±0.08	11.6±0.1 (EI)[c]
	12.2 ±0.3 (2nd)	
CH_4N^+	11.9 ±0.02	—

PI, PE, and EI denote the methods of photoionization mass spectrometry, electron impact mass spectrometry, and photoelectron spectroscopy, respectively. a) Ref. 15. b) Ref. 12. c) Ref. 8.

energy up to the marked photon energy.

The ionization energy of the parent ion and the appearance energies of the four fragment ions were determined from the ionization efficiency curves (Fig. 2) and are listed in Table 1 with the reference data.

Metastable peak at m/z ca. 26.5 due to slow fragmentation of m/z 73→44[16] was observed in the 30 eV electron impact ionization. The other metastable peak implying a successive reaction, m/z 73→58→30, is also observed at m/z ca. 15.5 due to m/z 58→30.

Discussion

The appearance energy (9.12±0.06 eV) of the parent ion, m/z 73, is agreed well with the value of an adiabatic ionization energy determined by PES.[7] Mass numbers of the fragment ions, m/z 72, 58, and 44, are assigned to $C_2H_6NO^+$, $C_2H_4NO^+$, and $C_2H_6N^+$, respectively (see Fig. 4). All of three fragment ions except for m/z 30 are produced in the unimolecular decompositions of the parent ion m/z 73, Eqs. 1—3.

$$C_3H_7NO^{+\cdot} \rightarrow C_2H_6N^+(44) + {\cdot}CHO \quad (1)$$

$$\rightarrow C_2H_4NO^+(58) + {\cdot}CH_3 \quad (2)$$

$$\rightarrow C_2H_6NO^+(72) + H \quad (3)$$

***m/z*=44.** The m/z 44 appears at 10.59±0.07 eV of photon energy and grows rapidly from ca. 1.5 eV above the appearance energy. The intensity ratios of m/z 44 against m/z 72 and 58 did not change so much up to ca. 12 eV of photon energy. The appearance of $C_2H_6N^+$ at 10.59 eV was not detected previously by mean of electron impact ionization. Meanwhile, the second rise at

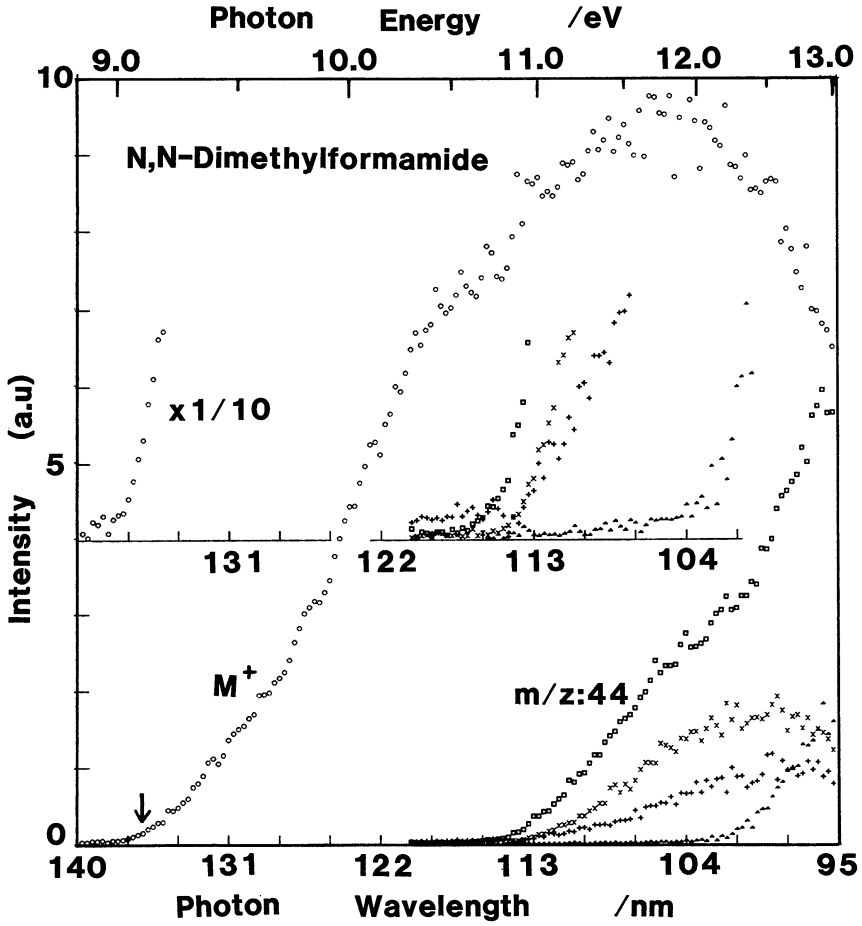

Fig. 2. The photo-ionization efficiency curves of *N,N*-dimethylformamide ion and three fragment ions. Each ions are denoted by ○: the parent ion m/z 73$^+$, +: m/z 72 ($C_3H_6NO^+$), ×: m/z 58 ($C_2H_4NO^+$), □: m/z 44 ($C_2H_6N^+$), ▲: m/z 30 (CH_4N^+).

12.2±0.3 eV is rather close to the previously reported appearance energy of $C_2H_6N^+$ by electron impact.[8] The second rise for m/z 44 in the RI curve (Fig. 3) indicates the appearance of another process at the photon energy above 12.2 eV. Four kinds of process are candidates or another fragmentation to m/z 44; (i) the fragments in Eq. 1 have high KER, (ii) the fragment ion is in an electronically excited state as given in Eq. 4, (iii) the fragment neutral is in an electronically excited state as is given in Eq. 5, (iv) the total enthalpy of the products by the successive reaction is so large as is given in Eq. 6.

$$C_3H_7NO^{+\cdot}* \rightarrow C_2H_6N^+(m/z\ 44)+CHO\cdot \quad (4)$$

$$\rightarrow C_2H_6N^+ + CHO\cdot* \quad (5)$$

$$\rightarrow C_2H_6N^+ + H + CO \quad (6)$$

Here, the asterisk denotes the species in an excited state. The processes Eqs. 4—6 are not clear from the energetic point of view. Alternative assignment of m/z 44 as $C_2H_4^+$ having the same mass number as $C_2H_6N^+$ is not coincided with the high resolution mass spectrum (electron impact) obtained. The fragments produced by electron impact are assumed not to be so different from those produced by photoionization. The sum of enthalpy ($\Sigma\Delta H_f$) of the products is not estimated for Eq. 4, because the excitation energies of $C_2H_6N^{+}*$ are unknown. The product CHO·* in Eq. 5 has excited electronic states at 1.15 eV and 3.0 eV[9] above the ground state. The first excitation energy of CHO·, 1.15 eV, is lower than ca. 1.5 eV which is the energy difference between the appearance energy and the second rise of m/z 44. The sum of enthalpy for CO and H[17] (1.11 eV), which are the products in Eq. 3, is larger than the ΔH_f of CHO· by 0.94 eV. This difference in energy is smaller than the difference of ca. 1.5 eV obtained.

Formations of high energetic products such as CHO·* in the excited electronic state or a pair of CO and H substantially reduce their kinetic energy released (KER) of $C_2H_6N^+$ compared with the formation of $C_2H_6N^+$ via the first decomposition channel. Effects of the ion repeller voltage on the intensity of $C_2H_6N^+$ and of the parent ion were measured as are shown in Figs. 5 (a) and (b) in place for direct measurement of KER. For the

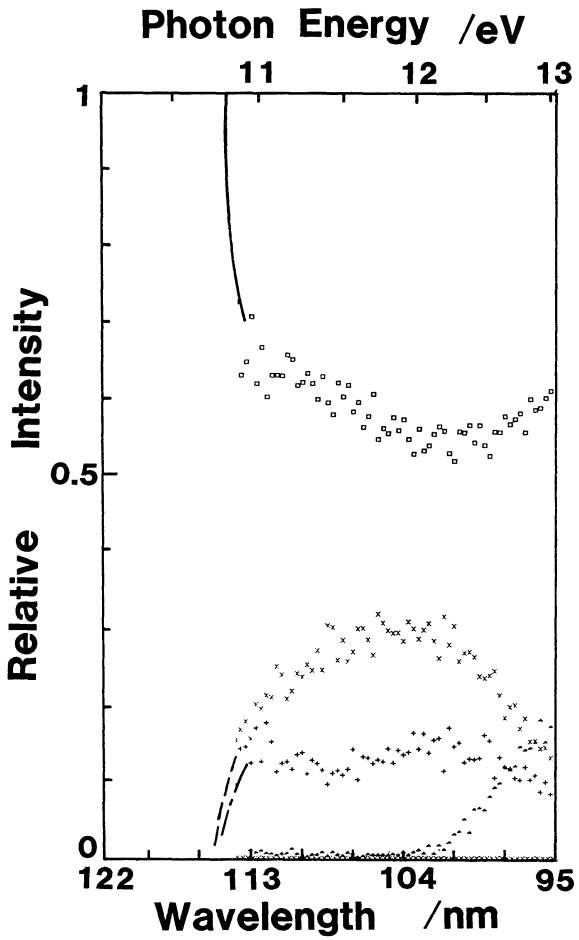

Fig. 3. The relative intensity curve normalized by the sum of four fragment ions (breakdown curves). Each ions are denoted by +: m/z 72 ($C_3H_6NO^+$), ×: m/z 58 ($C_2H_6NO^+$), □: m/z 44 ($C_2H_6N^+$), ▲: m/z 30 (CH_4N^+).

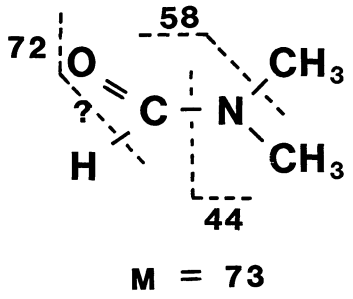

Fig. 4. The molecular structure of *N,N*-dimethylformamide. The dotted lines show the scheme of bonds rupture to produce the fragment ions.

sake of comparison, the dependence of ion repeller voltage on the intensities of $C_2H_5Br^{+\cdot}$ and of $C_2H_5^+$ are shown in Figs. 5 (c) and (d) for a fragmentation, $C_2H_5Br^{+\cdot} \rightarrow C_2H_5^+ + \cdot Br$, where $C_2H_5^+$ is known to have a higher KER than that partitioned statistically above 12.0 eV excitation.[10] At lower repeller voltages, the higher relative intensity of $C_2H_6N^+$ than the parent ion obtained on the 13.0 eV excitation implies a higher KER of $C_2H_6N^+$ as in the case of $C_2H_5^+$. The high KER of $C_2H_6N^+$ is inconsistent with Eqs. 4—6. Therefore, m/z 73 on the excitation above 12.2 eV decomposes along a repulsive potential to give $C_2H_6N^+$ with a high KER.

High energy electron impact ionization (30 eV) produces a metastable peak at m/z 26.5 due to fragmentation, M^+ (73)→44^+ as is shown in Fig. 6. The slow fragmentation giving the metastable peak at m/z 26.5 can not be ascribed to DMF^+ formed on the lower excitation energy than 12.2 eV, because the rate of the fragmentation to m/z 44 is the greatest among those to m/z 44, 58, and 72 assuming from the greatest intensity. Most probably, the slow fragmentation rises from an electronically excited DMF^+ formed on the high excitation energy. The metastable peak at m/z 26.5 suggests that the DMF^+ in the excited electronic state having a high vibrational energy takes the long way round before crossing the potential to dissociate. The second process producing $C_2H_6N^+$ presumably takes place along a repulsive potential after the slow crossing.

Fig. 7 shows a schematic energy diagram of $C_3H_7NO^{+\cdot}$ with its PES and the ionization efficiency curve of $C_2H_6N^+$. The point D indicates the lowest energy level of $C_3H_7NO^{+\cdot}$ dissociating to $C_2H_6N^+$ and CHO·. The parent ion excited above the threshold energy B stretches the N–C bond to dissociate. The transition probability to a hatched part above level B is very small, which is in agreement with the efficiencies of photoelectron and the photoionization efficiency curves. The transition probability to a repulsive energy level is also very small. The parent ion is efficiently excited to an energy level C by a vertical transition shown by a big arrow in PES. The formation of $C_2H_6N^+$ and CHO· in the ground state occurs at an intersystem-crossing point (C) between a bonding and an antibonding potential curve. After some vibrational relaxation the parent ion in the excited electronic state decomposes along the repulsive potential. The major part of the energy difference between the intersystem-crossing point and the dissociation limit D is converted to the kinetic energies of the dissociation products.

***m/z*=30.** The RI curve for m/z 30 arises in place of m/z 58 coming down. The m/z 30 is assigned to CH_4N^+ over NO^+ (m/z 30 produced from CH_3NO_2 by help of high resolution mass spectrum.)

$$C_3H_7NO^{+\cdot *} \rightarrow (C_2H_4NO^+) \rightarrow CH_4N^{+\cdot} + CO + \cdot CH_3 \quad (7)$$

This CH_4N^+ produced from DMF^+ is also discriminated from both CH_2O^+ and $C_2H_6^+$ having the same m/z 30. This assignment is supported by the $\Sigma\Delta H_f$ of the decomposition products in the following alternative reactions.

The formation of $CH_4N^{+\cdot}$ together with CO (Eq. 7) is supported by the $\Sigma\Delta H_f$ of the decomposition products. The sum of enthalpy is calculated to be 8.0 eV, which is

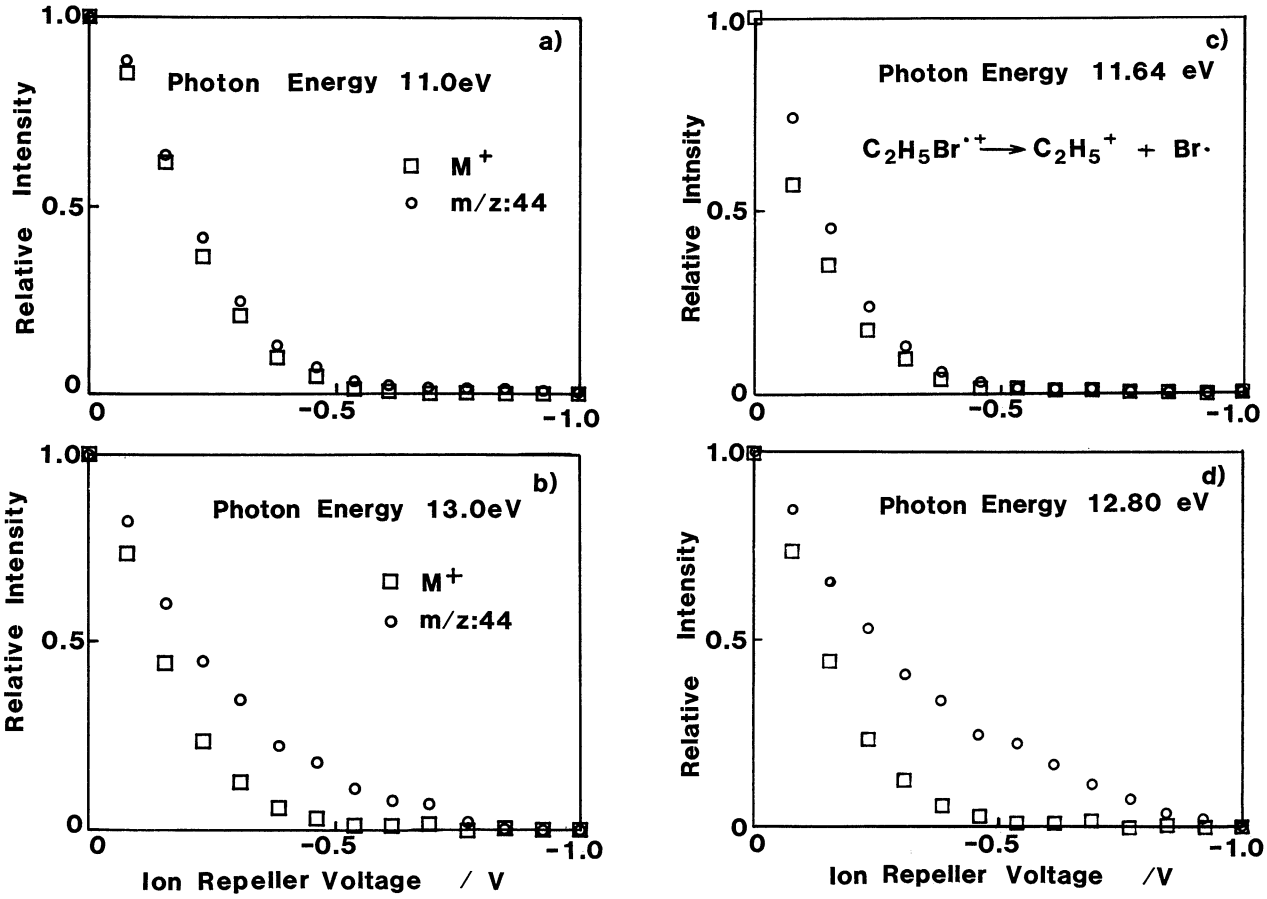

Fig. 5. The dependence of m/z 44 (○) and parent ion (□) on the reverse ion repeller voltages at the photon energy 11.0 eV (a) and 13.0 eV (b). The dependence of $C_2H_5^+$ (○) eliminated from ethyl bromide ion (□) at the photon energy 12.8 eV (c) and 11.64 eV (d) on the reverse ion repeller voltages. Since the ionization still occurs via the first channel in the higher photon energy region than ca. 12.2 eV, even if the new channel occurs through one of the processes such as Eqs. 1—3, the average KER of $C_2H_6NO^+$ will not drop significantly.

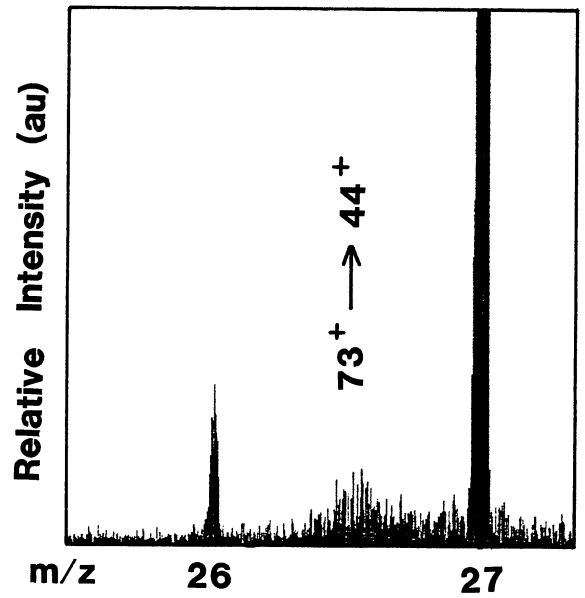

Fig. 6. A metastable peak at m/z ca. 26.5 corresponds to the fragmentation, $73^+ \rightarrow 44^+$, by 30 eV electron impact.

lower than the activation potential (9.9 eV[18]) estimated from the appearance energy (11.9 eV) for m/z 30. For alternative fragmentation processes, Eqs. 8—10 are followings.

$$C_3H_7NO^{+\cdot}* \rightarrow (C_2H_4NO^+) \rightarrow NO^{+\cdot} + C_2H_4 + \cdot CH_3 \quad (8)$$

$$\rightarrow CH_2O^{+\cdot} + CH_2N + \cdot CH_3 \quad (9)$$

$$\cdots\cdots\cdots\rightarrow C_2H_6^{+\cdot} + CHNO \quad (10)$$

The $\Sigma\Delta H$ are estimated to be 12.2,>11.2, and >10.8 eV, respectively, which are larger than the activation potential of the process giving m/z 30.

The appearance of fragment ions, $C_3H_6NO^+$, $C_2H_4NO^+$, and $C_2H_6N^+$, at the similar energies (Table 1) may be realized by ionization mechanism (kinetics and/or energetics). The small transition probability at the appearance energies makes the onsets of the ionization efficiency curves ambiguous. A tentative explanation is as follows. DMF is ionized above 9.12 eV via the

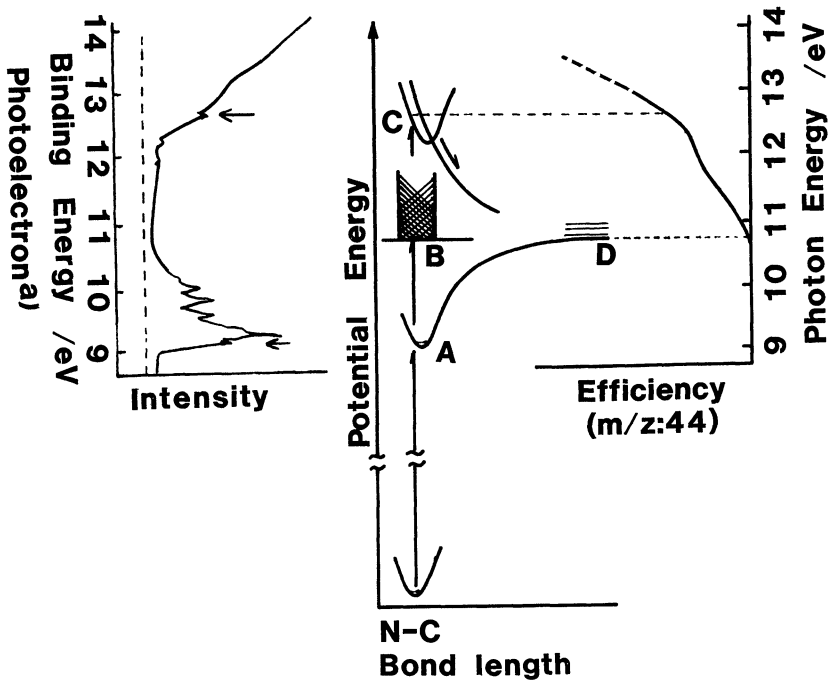

Fig. 7. The schematic energy diagram of fragmentation of *N,N*-dimethylformamide ion with the PES and the breakdown curve of m/z 44. The arrow in the PES points the vertical ionization energy A. *N,N*-dimethylformamide is excited vertically in the higher energy region than 10.7 eV of its continuum energy level B in producing CHO· and $C_2H_6N^+$ at D. A predissociative ionization producing CHO· occurs at C (ca. 12.2 eV) corresponding to a peak in the PES which is pointed by the big arrow.

removal of nonbonding electron of the nitrogen and/or the oxygen atom.[11] The ionization mechanism suggests that the removal of a nonbonding electron causes a change in the molecular orbital hybridization from sp^3 to sp^2 on the nitrogen atom of $C_3H_7NO^{+\cdot}$[12] accompanied by reduction of the length of C–N and the bond angle of C–N–C and C–N–O. This brings about a conversion of the electronic energy to the internal vibrational and rotational energy for the parent ion. The increased internal energy of $C_3H_7NO^{+\cdot}$ exceeds the activation energy of the decompositions to $C_3H_6NO^+$, $C_2H_4NO^+$, or $C_2H_6N^+$. This seems to be one of the reasons why the appearance energies of three fragment ions are nearly the same, though the bond energies may be different from each other.

We thank Professor Takesi Ohno of Osaka University for his discussions on the kinetics.

References

1) H. M. Rosenstock, K. Draxl, B. W. Steiner, and J. T. Herron, "J. P. Chem. Ref. Data," NBS, (1976), Vol. 6.

2) W. Forst, "Theory of Unimolecular Reactions," Academic Press, New York (1973).

3) C. W. Tsang and A. G. Harrison, *Org. Mass Spectrom.*, **7**, 377 (1973). A. N. H. Yeo and D. H. Williams, *J. Am. Chem. Soc.*, **93**, 395 (1971).

4) M. T. Bowers et al., "Gas Phase Ion Chemistry," Academic Press, New York (1974), Vol. 1.

5) M. Arimura and Y. Yoshikawa, *Mass Spectrom. Jpn.*, **32**, 375 (1984).

6) J. Momigny, C. Goffart, and L. d'Or, *Int. J. Mass Spectrom. Ion Phys.*, **1**, 53 (1968).

7) G. W. Mines and H. W. Tompson, *Spectrochim. Acta, Part A*, **31**, 137 (1975).

8) B. G. Gowenlock, P. P. Jones, and J. R. Majer, *Trans. Faraday Soc.*, **57**, 23 (1961).

9) G. Herzberg, "Molecular Spectra and Molecular Structure, III. Electronic Spectra and Electronic Structure of Polyatomic Molecules," Van Nostrand-Reinhold, New York (1966).

10) M. T. Bowers, "Advanced Mass Spectrometry, A," p. 533 (1985).

11) D. A. Sweigart and D. W. Turner, *J. Am. Chem. Soc.*, **94**, 5592 (1972).

12). D. W. Turner, C. Baker, A. D. Baker, and C. R. Brundle, "Molecular Photoelectron Spectroscopy," John Wiley & Sons, New York (1970).

13) R. G. Cooks, J. H. Beynon, R. M. Capriol, and R. G. Lester, "Metastable Ions," Elsevier, New York (1973).

14) "Kagaku Binran," 3rd ed, ed by Chem. Soc. Jpn., Maruzen, Tokyo (1984).

15) K. Watanabe, T. Nakayama, and J. Mottl, *J. Quant. Spectrosc. Radiat. Transfer*, **2**, 369 (1962).

16) The mass number of metastable peak m due to the reaction $m_1 \rightarrow m_2^+ + n$ before the magnetic sector of mass spectrometer is given as follows.[a]

$m^*=m_2^2/m_1$

[a] Ref. 13.

17) The ΔH_f of respective species[a] are the followings in kcal mol^{-1}.

Species	$C_3H_7NO^{+\cdot}$	$NO^{+\cdot}$	CH_4N^+	$CH_2O^{+\cdot}$	$C_2H_6^{+\cdot}$
ΔH_{f298}	165	235	178	224	249
Species	C_2H_4	CO	$\cdot CH_3$	H	HCO
ΔH_{f298}	12.5	−26.4	34.0	52.1	8

The ΔH_f of $C_2H_4NO^+$, which is unknown, can be estimated from the appearance energy of $C_2H_4NO^+$ by using the following relation.

$$\Delta H_f(C_2H_4NO^+)+\Delta H_f(\cdot CH_3)\leqslant AE(C_2H_4NO^+) - IE(C_3H_7NO^{+\cdot})+\Delta H_f(C_3H_7NO^{+\cdot})$$

Where AE and IE are an appearance energy and an ionization energy, respectively. The enthalpy of $C_2H_4NO^+$ is estimated to $\leqslant$169 kcal mol^{-1}.

[a] Ref. 1, Ref. 14, Ref. 11.

18) Under the conservation of energy and momentum, the released energy from the parent ion is partitioned into the fragmentation products in a decomposition. The fragment ions, $C_2H_6N^+$ and $C_2H_5^+$, get about 40 and 73% of the respective whole released kinetic energy.